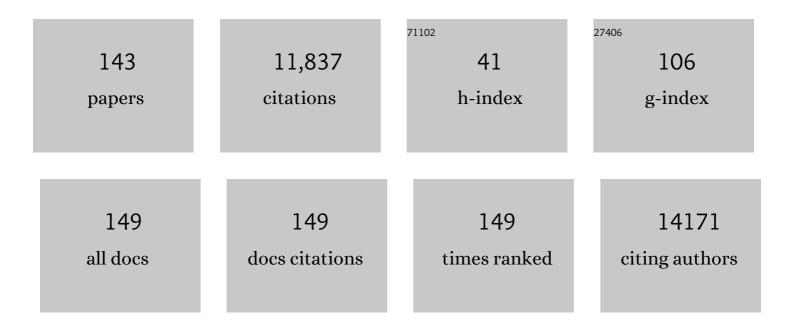
List of Publications by Year in descending order

Source: https://exaly.com/author-pdf/1941423/publications.pdf Version: 2024-02-01



Ρλιμ Μ/ Βομν

#	Article	IF	CITATIONS
1	Potential dependent spectroelectrochemistry of electrofluorogenic dyes on indiumâ€ŧin oxide. Electrochemical Science Advances, 2022, 2, e2100094.	2.8	5
2	Spatiotemporal distribution of chemical signatures exhibited by Myxococcus xanthus in response to metabolic conditions. Analytical and Bioanalytical Chemistry, 2022, 414, 1691-1698.	3.7	0
3	Coupling of 3D Porous Hosts for Li Metal Battery Anodes with Viscous Polymer Electrolytes. Journal of the Electrochemical Society, 2022, 169, 010511.	2.9	2
4	Real-time image denoising of mixed Poisson–Gaussian noise in fluorescence microscopy images using ImageJ. Optica, 2022, 9, 335.	9.3	27
5	Electrochemical Zero-Mode Waveguide Potential-Dependent Fluorescence of Glutathione Reductase at Single-Molecule Occupancy. Analytical Chemistry, 2022, 94, 3970-3977.	6.5	8
6	Potential-induced wetting and dewetting in hydrophobic nanochannels for mass transport control. Current Opinion in Electrochemistry, 2022, 34, 100980.	4.8	2
7	Redox cycling-based detection of phenazine metabolites secreted from <i>Pseudomonas aeruginosa</i> in nanopore electrode arrays. Analyst, The, 2021, 146, 1346-1354.	3.5	10
8	Biopolymer Patterning-Directed Secretion in Mucoid and Nonmucoid Strains of <i>Pseudomonas aeruginosa</i> Revealed by Multimodal Chemical Imaging. ACS Infectious Diseases, 2021, 7, 598-607.	3.8	4
9	Depth distributions of signaling molecules in Pseudomonas aeruginosa biofilms mapped by confocal Raman microscopy. Journal of Chemical Physics, 2021, 154, 204201.	3.0	3
10	Electrochemical Immunosensing of Interleukin-6 in Human Cerebrospinal Fluid and Human Serum as an Early Biomarker for Traumatic Brain Injury. ACS Measurement Science Au, 2021, 1, 65-73.	4.4	17
11	Actively Controllable Solid-Phase Microextraction in a Hierarchically Organized Block Copolymer-Nanopore Electrode Array Sensor for Charge-Selective Detection of Bacterial Metabolites. Analytical Chemistry, 2021, 93, 14481-14488.	6.5	5
12	Potential-induced wetting and dewetting in pH-responsive block copolymer membranes for mass transport control. Faraday Discussions, 2021, 233, 283-294.	3.2	2
13	Electrochemical and spectroelectrochemical characterization of bacteria and bacterial systems. Analyst, The, 2021, 147, 22-34.	3.5	10
14	Silver Nanofilament Formation Dynamics in a Polymerâ€ŀonic Liquid Thin Film by Direct Write. Advanced Functional Materials, 2020, 30, 1907950.	14.9	4
15	lon Gating in Nanopore Electrode Arrays with Hierarchically Organized pH-Responsive Block Copolymer Membranes. ACS Applied Materials & Interfaces, 2020, 12, 55116-55124.	8.0	20
16	Spatiotemporal Distribution of Pseudomonas aeruginosa Alkyl Quinolones under Metabolic and Competitive Stress. MSphere, 2020, 5, .	2.9	14
17	Acid–base chemistry at the single ion limit. Chemical Science, 2020, 11, 10951-10958.	7.4	9
18	Single Entity Electrochemistry in Nanopore Electrode Arrays: Ion Transport Meets Electron Transfer in Confined Geometries. Accounts of Chemical Research. 2020. 53. 719-728.	15.6	50

#	Article	IF	CITATIONS
19	Electrowettingâ€Mediated Transport to Produce Electrochemical Transistor Action in Nanopore Electrode Arrays. Small, 2020, 16, e1907249.	10.0	8
20	Microscale and Nanoscale Electrophotonic Diagnostic Devices. Cold Spring Harbor Perspectives in Medicine, 2019, 9, a034249.	6.2	2
21	Emerging Directions in Electroanalysis. Journal of Analysis and Testing, 2019, 3, 123-124.	5.1	0
22	Tunable optical metamaterial-based sensors enabled by closed bipolar electrochemistry. Analyst, The, 2019, 144, 6240-6246.	3.5	8
23	Whole-cell biosensing by siderophore-based molecular recognition and localized surface plasmon resonance. Analytical Methods, 2019, 11, 296-302.	2.7	18
24	Detection of 1†zmol injection of angiotensin using capillary zone electrophoresis coupled to a Q-Exactive HF mass spectrometer with an electrokinetically pumped sheath-flow electrospray interface. Talanta, 2019, 204, 70-73.	5.5	26
25	Electrochemical Surface-Enhanced Raman Spectroscopy of Pyocyanin Secreted by <i>Pseudomonas aeruginosa</i> Communities. Langmuir, 2019, 35, 7043-7049.	3.5	24
26	Nanopore-Templated Silver Nanoparticle Arrays Photopolymerized in Zero-Mode Waveguides. Frontiers in Chemistry, 2019, 7, 216.	3.6	4
27	Capture of Single Silver Nanoparticles in Nanopore Arrays Detected by Simultaneous Amperometry and Surface-Enhanced Raman Scattering. Analytical Chemistry, 2019, 91, 4568-4576.	6.5	16
28	Spatiotemporal dynamics of molecular messaging in bacterial co-cultures studied by multimodal chemical imaging. , 2019, 10863, .		5
29	(Invited) Closed Bipolar Electrochemistry with Multiplex Optical Readout for Rapid Diagnostics of Sepsis Syndrome Biomarkers. ECS Meeting Abstracts, 2019, , .	0.0	0
30	Zero-mode waveguide nanophotonic structures for single molecule characterization. Journal Physics D: Applied Physics, 2018, 51, 193001.	2.8	22
31	Quantitative SIMS Imaging of Agar-Based Microbial Communities. Analytical Chemistry, 2018, 90, 5654-5663.	6.5	30
32	Voltageâ€Gated Nanoparticle Transport and Collisions in Attoliterâ€Volume Nanopore Electrode Arrays. Small, 2018, 14, e1703248.	10.0	17
33	Nanopore Electrochemistry: A Nexus for Molecular Control of Electron Transfer Reactions. ACS Central Science, 2018, 4, 20-29.	11.3	48
34	Whole-Cell <i>Pseudomonas aeruginosa</i> Localized Surface Plasmon Resonance Aptasensor. Analytical Chemistry, 2018, 90, 2326-2332.	6.5	59
35	In Situ Probing of Laser Annealing of Plasmonic Substrates with Surface-Enhanced Raman Spectroscopy. Journal of Physical Chemistry C, 2018, 122, 11031-11037.	3.1	7
36	Spatially dependent alkyl quinolone signaling responses to antibiotics in Pseudomonas aeruginosa swarms. Journal of Biological Chemistry, 2018, 293, 9544-9552.	3.4	33

#	Article	IF	CITATIONS
37	Electrochemical Zero-Mode Waveguide Studies of Single Enzyme Reactions. , 2018, 2018, .		0
38	Surface-Growing Communities of Pseudomonas aeruginosa Exhibit Distinct Alkyl Quinolone Signatures. Microbiology Insights, 2018, 11, 117863611881773.	2.0	7
39	Redox Cycling in Individually Encapsulated Attoliter-Volume Nanopores. ACS Nano, 2018, 12, 12923-12931.	14.6	13
40	Processes at nanopores and bio-nanointerfaces: general discussion. Faraday Discussions, 2018, 210, 145-171.	3.2	3
41	Asymmetric Nafion-Coated Nanopore Electrode Arrays as Redox-Cycling-Based Electrochemical Diodes. ACS Nano, 2018, 12, 9177-9185.	14.6	24
42	Science and technology of electrochemistry at nano-interfaces: concluding remarks. Faraday Discussions, 2018, 210, 481-493.	3.2	5
43	Directâ€Write Formation and Dissolution of Silver Nanofilaments in Ionic Liquidâ€Polymer Electrolyte Composites. Small, 2018, 14, 1802023.	10.0	4
44	Nanopore-Organized Nanoparticle Arrays for Tunable Optical Materials Using Nanobioplar Electrodeposition. ECS Meeting Abstracts, 2018, , .	0.0	0
45	Spatial Mapping of Pyocyanin in <i>Pseudomonas Aeruginosa</i> Bacterial Communities Using Surface Enhanced Raman Scattering. Applied Spectroscopy, 2017, 71, 215-223.	2.2	34
46	Optical Biosensing of Bacteria and Bacterial Communities. Journal of Analysis and Testing, 2017, 1, 1.	5.1	21
47	Addressable Direct-Write Nanoscale Filament Formation and Dissolution by Nanoparticle-Mediated Bipolar Electrochemistry. ACS Nano, 2017, 11, 4976-4984.	14.6	20
48	Single-molecule spectroelectrochemical cross-correlation during redox cycling in recessed dual ring electrode zero-mode waveguides. Chemical Science, 2017, 8, 5345-5355.	7.4	36
49	Ion selective redox cycling in zero-dimensional nanopore electrode arrays at low ionic strength. Nanoscale, 2017, 9, 5164-5171.	5.6	26
50	Electrochromic Sensor for Multiplex Detection of Metabolites Enabled by Closed Bipolar Electrode Coupling. ACS Sensors, 2017, 2, 1020-1026.	7.8	59
51	Nanochannel Arrays for Molecular Sieving and Electrochemical Analysis by Nanosphere Lithography Templated Graphoepitaxy of Block Copolymers. ACS Applied Materials & Interfaces, 2017, 9, 24908-24916.	8.0	17
52	A Carotenoid-Deficient Mutant in Pantoea sp. YR343, a Bacteria Isolated from the Rhizosphere of Populus deltoides, Is Defective in Root Colonization. Frontiers in Microbiology, 2016, 7, 491.	3.5	48
53	Coupling of Independent Electrochemical Reactions and Fluorescence at Closed Bipolar Interdigitated Electrode Arrays. ChemElectroChem, 2016, 3, 422-428.	3.4	36
54	Label-free molecular imaging of bacterial communities of the opportunistic pathogen Pseudomonas aeruginosa. , 2016, 9930, .		12

#	Article	IF	CITATIONS
55	From single cells to single molecules: general discussion. Faraday Discussions, 2016, 193, 141-170.	3.2	4
56	Metal-assisted polyatomic SIMS and laser desorption/ionization for enhanced small molecule imaging of bacterial biofilms. Biointerphases, 2016, 11, 02A325.	1.6	21
57	Microchannel Voltammetry in the Presence of Large External Voltages and Electric Fields. Analytical Chemistry, 2016, 88, 4200-4204.	6.5	2
58	Electrochemistry at single molecule occupancy in nanopore-confined recessed ring-disk electrode arrays. Faraday Discussions, 2016, 193, 51-64.	3.2	29
59	Closed bipolar electrode-enabled dual-cell electrochromic detectors for chemical sensing. Analyst, The, 2016, 141, 6018-6024.	3.5	31
60	Redox Cycling in Nanopore-Confined Recessed Dual-Ring Electrode Arrays. Journal of Physical Chemistry C, 2016, 120, 20634-20641.	3.1	30
61	Effects of molecular confinement and crowding on horseradish peroxidase kinetics using a nanofluidic gradient mixer. Lab on A Chip, 2016, 16, 877-883.	6.0	5
62	Ion Accumulation and Migration Effects on Redox Cycling in Nanopore Electrode Arrays at Low Ionic Strength. ACS Nano, 2016, 10, 3658-3664.	14.6	47
63	Raman chemical imaging of the rhizosphere bacterium Pantoea sp. YR343 and its co-culture with Arabidopsis thaliana. Analyst, The, 2016, 141, 2175-2182.	3.5	30
64	Nanopore-enabled electrode arrays and ensembles. Mikrochimica Acta, 2016, 183, 1019-1032.	5.0	18
65	Single occupancy spectroelectrochemistry of freely diffusing flavin mononucleotide in zero-dimensional nanophotonic structures. Faraday Discussions, 2015, 184, 101-115.	3.2	41
66	Self-induced redox cycling coupled luminescence on nanopore recessed disk-multiscale bipolar electrodes. Chemical Science, 2015, 6, 3173-3179.	7.4	36
67	On-demand in situ generation of oxygen in a nanofluidic embedded planar microband electrochemical reactor. Microfluidics and Nanofluidics, 2015, 19, 1181-1189.	2.2	10
68	Using Raman spectroscopy and SERS for in situ studies of rhizosphere bacteria. , 2015, 9550, .		1
69	Multimodal chemical imaging of molecular messengers in emerging Pseudomonas aeruginosa bacterial communities. Analyst, The, 2015, 140, 6544-6552.	3.5	58
70	Electric field effects on current–voltage relationships in microfluidic channels presenting multiple working electrodes in the weak-coupling limit. Microfluidics and Nanofluidics, 2015, 18, 131-140.	2.2	9
71	Tunable electrochemical pH modulation in a microchannel monitored via the proton-coupled electro-oxidation of hydroquinone. Biomicrofluidics, 2014, 8, 044120.	2.4	15
72	Coupled Electrokinetic Transport and Electron Transfer at Annular Nanoband Electrodes Embedded in Cylindrical Nanopores. ChemElectroChem, 2014, 1, 1570-1576.	3.4	9

#	Article	IF	CITATIONS
73	Correlated Imaging with C <sub>60</sub> -SIMS and Confocal Raman Microscopy: Visualization of Cell-Scale Molecular Distributions in Bacterial Biofilms. Analytical Chemistry, 2014, 86, 10885-10891.	6.5	58
74	Correlated mass spectrometry imaging and confocal Raman microscopy for studies of three-dimensional cell culture sections. Analyst, The, 2014, 139, 4578.	3.5	61
75	Spatial organization of Pseudomonas aeruginosa biofilms probed by combined matrix-assisted laser desorption ionization mass spectrometry and confocal Raman microscopy. Analyst, The, 2014, 139, 5700-5708.	3.5	42
76	Potential-Dependent Restructuring and Chemical Noise at Au–Ag–Au Atomic Scale Junctions. ACS Nano, 2014, 8, 1718-1727.	14.6	4
77	Redox Cycling on Recessed Ring-Disk Nanoelectrode Arrays in the Absence of Supporting Electrolyte. Journal of the American Chemical Society, 2014, 136, 7225-7228.	13.7	52
78	MALDI-guided SIMS: Multiscale Imaging of Metabolites in Bacterial Biofilms. Analytical Chemistry, 2014, 86, 9139-9145.	6.5	79
79	Recessed Ring–Disk Nanoelectrode Arrays Integrated in Nanofluidic Structures for Selective Electrochemical Detection. Analytical Chemistry, 2013, 85, 9882-9888.	6.5	49
80	Potential-dependent single molecule blinking dynamics for flavin adenine dinucleotide covalently immobilized in zero-mode waveguide array of working electrodes. Faraday Discussions, 2013, 164, 57.	3.2	39
81	Nanofluidics: Convective Delivery of Electroactive Species to Annular Nanoband Electrodes Embedded in Nanocapillary-Array Membranes (Small 1/2013). Small, 2013, 9, 164-164.	10.0	0
82	Correlated imaging – a grand challenge in chemical analysis. Analyst, The, 2013, 138, 1924.	3.5	56
83	Redox Cycling in Nanoscale-Recessed Ring-Disk Electrode Arrays for Enhanced Electrochemical Sensitivity. ACS Nano, 2013, 7, 5483-5490.	14.6	99
84	Chemical Noise Produced by Equilibrium Adsorption/Desorption of Surface Pyridine at Au–Ag–Au Bimetallic Atom-Scale Junctions Studied by Fluctuation Spectroscopy. Journal of the American Chemical Society, 2013, 135, 4522-4528.	13.7	12
85	Convective Delivery of Electroactive Species to Annular Nanoband Electrodes Embedded in Nanocapillaryâ€Array Membranes. Small, 2013, 9, 90-97.	10.0	13
86	Non-aqueous microchip electrophoresis for characterization of lipid biomarkers. Interface Focus, 2013, 3, 20120096.	3.0	12
87	Catalyst and processing effects on metal-assisted chemical etching for the production of highly porous GaN. Semiconductor Science and Technology, 2013, 28, 065001.	2.0	21
88	lonic transport in nanocapillary membrane systems. , 2012, , 17-31.		0
89	Single-Molecule Enzyme Dynamics of Monomeric Sarcosine Oxidase in a Gold-Based Zero-Mode Waveguide. Applied Spectroscopy, 2012, 66, 163-169.	2.2	24
90	Monodisperse GaN nanowires prepared by metal-assisted chemical etching with in situ catalyst deposition. Electrochemistry Communications, 2012, 19, 39-42.	4.7	42

#	Article	IF	CITATIONS
91	Enhanced Mass Transport of Electroactive Species to Annular Nanoband Electrodes Embedded in Nanocapillary Array Membranes. Journal of the American Chemical Society, 2012, 134, 8617-8624.	13.7	46
92	Nanoporous Ag–GaN thin films prepared by metalâ€assisted electroless etching and deposition as threeâ€dimensional substrates for surfaceâ€enhanced Raman scattering. Journal of Raman Spectroscopy, 2012, 43, 1347-1353.	2.5	16
93	Conductance-Based Chemical Sensing in Metallic Nanowires and Metal-Semiconductor Nanostructures. Analytical Chemistry, 2012, 84, 2-8.	6.5	17
94	Ionic transport in nanocapillary membrane systems. Journal of Nanoparticle Research, 2012, 14, 1.	1.9	19
95	Fabrication of antireflective layers on silicon using metal-assisted chemical etching with in situ deposition of silver nanoparticle catalysts. Solar Energy Materials and Solar Cells, 2012, 103, 98-107.	6.2	52
96	Robust Au–Ag–Au Bimetallic Atom-Scale Junctions Fabricated by Self-Limited Ag Electrodeposition at Au Nanogaps. ACS Nano, 2011, 5, 8434-8441.	14.6	7
97	Electrolysis in nanochannels for in situ reagent generation in confined geometries. Lab on A Chip, 2011, 11, 3634.	6.0	30
98	Metal-Assisted Chemical Etching Using Tollen's Reagent to Deposit Silver Nanoparticle Catalysts for Fabrication of Quasi-ordered Silicon Micro/Nanostructures. Journal of Electronic Materials, 2011, 40, 2480-2485.	2.2	35
99	Effect of Molecular Adsorption on the Electrical Conductance of Single Au Nanowires Fabricated by Electronâ€Beam Lithography and Focused Ion Beam Etching. Small, 2010, 6, 2598-2603.	10.0	34
100	Electrochemical Control of Stability and Restructuring Dynamics in Auâ^'Agâ^'Au and Auâ^'Cuâ^'Au Bimetallic Atom-Scale Junctions. ACS Nano, 2010, 4, 2946-2954.	14.6	16
101	Spatial Correlation of Confocal Raman Scattering and Secondary Ion Mass Spectrometric Molecular Images of Lignocellulosic Materials. Analytical Chemistry, 2010, 82, 2608-2611.	6.5	41
102	Nanofluidics in chemical analysis. Chemical Society Reviews, 2010, 39, 1060-1072.	38.1	168
103	Electrokinetic control of fluid transport in gold-coated nanocapillary array membranes in hybrid nanofluidic–microfluidic devices. Lab on A Chip, 2010, 10, 1237.	6.0	18
104	High sensitivity hydrogen sensing with Pt-decorated porous gallium nitride prepared by metal-assisted electroless etching. Analyst, The, 2010, 135, 902.	3.5	27
105	Nanoscale Control and Manipulation of Molecular Transport in Chemical Analysis. Annual Review of Analytical Chemistry, 2009, 2, 279-296.	5.4	60
106	Enzymatic activity of surface-immobilized horseradish peroxidase confined to micrometer- to nanometer-scale structures in nanocapillary array membranes. Analyst, The, 2009, 134, 851.	3.5	18
107	Science and technology for water purification in the coming decades. , 2009, , 337-346.		110
108	Fluidic communication between multiple vertically segregated microfluidic channels connected by nanocapillary array membranes. Electrophoresis, 2008, 29, 1237-1244.	2.4	15

#	Article	IF	CITATIONS
109	Science and technology for water purification in the coming decades. Nature, 2008, 452, 301-310.	27.8	6,795
110	Electrokinetically driven fluidic transport in integrated three-dimensional microfluidic devices incorporating gold-coated nanocapillary array membranes. Lab on A Chip, 2008, 8, 1625.	6.0	19
111	Nanofluidics: Systems and Applications. IEEE Sensors Journal, 2008, 8, 441-450.	4.7	93
112	Perturbation of Microfluidic Transport Following Electrokinetic Injection through a Nanocapillary Array Membrane: Injection and Biphasic Recovery. Journal of Physical Chemistry C, 2008, 112, 19242-19247.	3.1	6
113	Stable Atom-Scale Junctions on Silicon Fabricated by Kinetically Controlled Electrochemical Deposition and Dissolution. ACS Nano, 2008, 2, 1581-1588.	14.6	14
114	Functional-DNA–Based Nanoscale Materials and Devices for Sensing Trace Contaminants in Water. MRS Bulletin, 2008, 33, 34-41.	3.5	16
115	Temperature-Controlled Flow Switching in Nanocapillary Array Membranes Mediated by Poly(N-isopropylacrylamide) Polymer Brushes Grafted by Atom Transfer Radical Polymerization. Langmuir, 2007, 23, 305-311.	3.5	157
116	Induced Electrokinetic Transport in Microâ^'Nanofluidic Interconnect Devices. Langmuir, 2007, 23, 13209-13222.	3.5	89
117	Surface Immobilization of Catalytic Beacons Based on Ratiometric Fluorescent DNAzyme Sensors:  A Systematic Study. Langmuir, 2007, 23, 9513-9521.	3.5	42
118	Incorporation of a DNAzyme into Au-coated nanocapillary array membranes with an internal standard for Pb(ii) sensing. Analyst, The, 2006, 131, 41-47.	3.5	65
119	Modeling and Simulation of Ionic Currents in Three-Dimensional Microfluidic Devices with Nanofluidic Interconnects. Journal of Nanoparticle Research, 2005, 7, 507-516.	1.9	54
120	Voltage-Tunable Volume Transitions in Nanoscale Films of Poly(hydroxyethyl methacrylate) Surfaces Grafted onto Gold. Langmuir, 2005, 21, 1979-1985.	3.5	33
121	Miniaturized Lead Sensor Based on Lead-Specific DNAzyme in a Nanocapillary Interconnected Microfluidic Device. Environmental Science & Technology, 2005, 39, 3756-3761.	10.0	123
122	Profiling pH Gradients Across Nanocapillary Array Membranes Connecting Microfluidic Channels. Journal of the American Chemical Society, 2005, 127, 13928-13933.	13.7	48
123	Interfacial Scattering at Electrochemically Fabricated Atom-Scale Junctions between Thin Gold Film Electrodes in a Microfluidic Channel. Analytical Chemistry, 2005, 77, 243-249.	6.5	23
124	Immobilization of a Catalytic DNA Molecular Beacon on Au for Pb(II) Detection. Analytical Chemistry, 2005, 77, 442-448.	6.5	119
125	Nanocapillary Arrays Effect Mixing and Reaction in Multilayer Fluidic Structures. Angewandte Chemie - International Edition, 2004, 43, 1862-1865.	13.8	42
126	Microfluidic Separation and Gateable Fraction Collection for Mass-Limited Samples. Analytical Chemistry, 2004, 76, 6419-6425.	6.5	63

#	Article	IF	CITATIONS
127	Surface Adsorption and Transfer of Organomercaptans to Colloidal Gold and Direct Identification by Matrix Assisted Laser Desorption/Ionization Mass Spectrometry. Journal of the American Chemical Society, 2004, 126, 5920-5926.	13.7	50
128	Direct-write patterning of microstructured porous silicon arrays by focused-ion-beam Pt deposition and metal-assisted electroless etching. Journal of Applied Physics, 2004, 96, 6888-6894.	2.5	69
129	Structural and spectroscopic characterization of porous silicon carbide formed by Pt-assisted electroless chemical etching. Solid State Communications, 2003, 126, 245-250.	1.9	65
130	Hybrid three-dimensional nanofluidic/microfluidic devices using molecular gates. Sensors and Actuators A: Physical, 2003, 102, 223-233.	4.1	105
131	Nanocapillary Array Interconnects for Gated Analyte Injections and Electrophoretic Separations in Multilayer Microfluidic Architectures. Analytical Chemistry, 2003, 75, 2224-2230.	6.5	101
132	Gateable Nanofluidic Interconnects for Multilayered Microfluidic Separation Systems. Analytical Chemistry, 2003, 75, 1861-1867.	6.5	204
133	Morphology evolution and luminescence properties of porous GaN generated via Pt-assisted electroless etching of hydride vapor phase epitaxy GaN on sapphire. Journal of Applied Physics, 2003, 94, 7526.	2.5	44
134	In-plane control of morphology and tunable photoluminescence in porous silicon produced by metal-assisted electroless chemical etching. Journal of Applied Physics, 2002, 91, 6134-6140.	2.5	164
135	In-plane bandgap control in porous GaN through electroless wet chemical etching. Applied Physics Letters, 2002, 80, 980-982.	3.3	102
136	Manipulating Molecular Transport through Nanoporous Membranes by Control of Electrokinetic Flow:A Effect of Surface Charge Density and Debye Length. Langmuir, 2001, 17, 6298-6303.	3.5	132
137	Direct assay ofAplysia tissues and cells with laser desorption/ionization mass spectrometry on porous silicon. Journal of Mass Spectrometry, 2001, 36, 1317-1322.	1.6	73
138	Chemisorption and Chemical Reaction Effects on the Resistivity of Ultrathin Gold Films at the Liquidâ 'Solid Interface. Analytical Chemistry, 1999, 71, 119-125.	6.5	55
139	Near-field photoluminescence of microcrystalline arsenic oxides produced in anodically processed gallium arsenide. Applied Physics Letters, 1999, 74, 1096-1098.	3.3	21
140	Inâ^'Plane Resistivity of Ultrathin Gold Films:  A High Sensitivity, Molecularly Differentiated Probe of Mercaptan Chemisorption at the Liquidâ^'Metal Interface. Journal of the American Chemical Society, 1998, 120, 9969-9970.	13.7	51
141	LOCALIZED OPTICAL PHENOMENA AND THE CHARACTERIZATION OF MATERIALS INTERFACES. Annual Review of Materials Research, 1997, 27, 469-498.	5.5	20
142	Optical determination of surface density in oriented metalloprotein nanostructures. Analytical Chemistry, 1993, 65, 1635-1638.	6.5	35
143	Genetic engineering of surface attachment sites yields oriented protein monolayers. Journal of the American Chemical Society, 1992, 114, 9298-9299.	13.7	70